In-Medium Effects on Particle Production in Heavy Ion Collisions

V. Prassa [a] G.Ferini [b] T. Gaitanos [c] H.H. Wolter [d]
G.A. Lalazissis [a] M. Di Toro [b]

[a] *Department of Theoretical Physics, Aristotle University of Thessaloniki, Thessaloniki Gr-54124,Greece*

[b] *Laboratori Nazionali del Sud INFN, I-95123 Catania, Italy*

[c] *Institut für Theoretische Physik, Justus-Liebig-Universität Giessen, D-35392 Giessen, Germany*

[d] *Sektion Physik, Universität München, D-85748 Garching, Germany*

email: Theodoros.Gaitanos@theo.physik.uni-giessen.de

The effect of possible in-medium modifications of nucleon-nucleon (NN) cross sections on particle production is investigated in heavy ion collisions (HIC) at intermediate energies. In particular, using a fully covariant relativistic transport approach, we see that the density dependence of the *inelastic* cross sections appreciably affects the pion and kaon yields and their rapidity distributions. However, the (π^-/π^+)- and (K^0/K^+)-ratios depend only moderately on the in-medium behavior of the inelastic cross sections. This is particularly true for kaon yield ratios, since kaons are more uniformly produced in high density regions. Kaon potentials are also suitably evaluated in two schemes, a chiral perturbative approach and an effective meson-quark coupling method, with consistent results showing a similar repulsive contribution for K^+ and K^0. As a consequence we expect rather reduced effects on the yield ratios. We conclude that particle ratios appear to be robust observables for probing the nuclear equation of state (EoS) at high baryon density and, particularly, its isovector sector.

Key words: Asymmetric nuclear matter, symmetry energy, relativistic heavy ion collisions, particle production.
PACS numbers: **25.75.-q**, **21.65.+f**, 21.30.Fe, 25.75.Dw.

1 Introduction

The knowledge of the properties of highly compressed and heated hadronic matter is an important issue for the understanding of astrophysical processes, such as the mechanism of supernovae explosions and the physics of neutron stars [1,2]. Heavy ion collisions provide the unique opportunity to explore highly excited hadronic matter, i.e. the high density behavior of the nuclear EoS, under controlled conditions (high baryon energy densities and temperatures) in the laboratory [3]. Of particular recent interest is also the still poorly known density dependence of the isovector channel of the EoS.

Suggested observables have been the nucleon collective flows [3,4] and the distributions of produced particles such as pions and, in particular, particles with strangeness (kaons) [5,6]. Because of the rather high energy threshold (E_{lab} = 1.56 GeV for Nucleon-Nucleon collisions), kaon production in HICs at energies in the range $0.8 - 1.8$ $AGeV$ is mainly due to secondary processes involving Δ resonances and pions (π). On the other hand, secondary processes require high baryon density. This explains why the kaon production around threshold is intimately connected to the high density stage of the nucleus-nucleus collision. Furthermore, the relatively large mean free path of positive charged (K^+) and neutral (K^0) kaons inside the hadronic environment causes hadronic matter to be transparent for kaons [7]. Therefore kaon yields and generally *strangeness ratios* have been proposed as important signals for the investigation of the high density behavior of the nuclear EoS. This idea, as firstly suggested by Aichelin and Ko [8], has been recently applied in HIC at intermediate energies in terms of strangeness ratios, e.g. the ratio of the kaon yields in Au+Au and C+C collisions [5,9]. In these studies it was found that this ratio is very sensitive to the stiffness of the nuclear EoS. Indeed comparisons with KaoS data [10] favored a soft behavior of the high density nuclear EoS, a statement which is particularly consistent with elliptic flow data of the FOPI collaboration [11].

The idea of studying particle ratios in HICs around the kinematical threshold has been recently applied in the determination of the isovector channel of the nuclear EoS, i.e. the high density dependence of the symmetry energy E_{sym}. It has turned out that particle ratios, such as (π^-/π^+) [12] or (K^0/K^+) [13–15], are sensitive to the stiffness of the symmetry energy and, in particular to the strength of the vector isovector field. However in medium effects on the kaon propagation have been neglected so far. Here we will test the robustness of the yield ratio against the inclusion and the variation of the corresponding kaon potentials. At the same time in Ref. [16] the role of the in-medium modifications of NN cross sections has been studied in terms of baryon and strangeness dynamics. It was found that the pion and kaon yields are sensitively influenced by the reduced effective NN cross sections for inelastic processes. Here we will

see that the kaon yield ratio appears robust even with respect to the density dependence of the in-medium inelastic NN cross sections, while at variance the pion ratio seems to be more sensitive.

The collision dynamics is rather complex and involves the nuclear mean field (EoS) and binary 2-body collisions. In the presence of a nuclear medium the treatment of binary collisions represents a non-trivial problem. The NN cross sections for elastic and inelastic processes, which are the crucial physical parameters here, are experimentally accessible only in free space and not for 2-body scattering at finite baryon density. Recent microscopic studies, based on the G-matrix approach, have shown a strong decrease of the elastic NN cross section [17,18] in a hadronic medium. These in-medium effects of the elastic NN cross section considerably influence the hadronic reaction dynamics [19]. Obviously the question arises whether similar in-medium effects of the *inelastic* NN cross sections may affect the reaction dynamics and, in particular, the production of particles (pions and kaons).

Furthermore, the strangeness propagation inside the nuclear medium is even more complex and involves the additional consideration of kaon mean field potentials in the dynamical description. This is an important issue when comparing with experimental kaon data [10]. In a Chiral Perturbation approach at the lowest order (ChPT Potentials), the kaon (antikaon) potential has an attractive scalar and a repulsive (attractive) vector part [20]. This leads to weakly repulsive (strongly attractive) potentials for kaons (antikaons) with corresponding scalar and vector kaon-nucleon coupling constants depending on the parametrization [20,21] accounted for. Similar results can be obtained in an effective meson-coupling model (OBE Potentials, in the RMF spirit), where the K-meson couplings are simply related to the nucleon-meson ones, in the spirit of ref. [22]. The latter approach has the advantage of being fully consistent with the covariant transport equations used to simulate the reaction dynamics [14,15]. We remind that the high density dependence of the kaon self energies is still an object of current debate, e.g. see Refs. [23,7] in which the role of the kaon potential has been investigated in terms of kaon in-plane and out-of-plane flows. Moreover for studies aimed to the determination of the symmetry energy from strangeness production one has to consider with particular care the isospin dependence of the kaon mean field potential.

The main focus of the present work is on a detailed study of the *robustness* of the pionic (π^-/π^+) and, in particular, the strangeness ratio (K^0/K^+) with respect to the in-medium modifications of the imaginary part of the nucleon self energy, i.e. the NN cross sections, and to the in-medium variations of the kaon self energy, i.e. the density dependence of the kaon potential. This analysis, which goes beyond our previous investigations of [14,15], is also motivated by new measurements of the FOPI collaboration [24] by means of the strangeness ratios.

The paper is organized as follows: The next Section describes the theoretical treatment of the reaction dynamics within the Relativistic Boltzmann-Uheling-Uhlenbeck (RBUU) transport equation. A detailed discussion on the in-medium modifications of the inelastic NN cross sections is presented. In Section 3 we discuss the kaon mean field potentials (in both ChPT and OBE/RMF schemes) and their expected isospin dependence. Section 4 is devoted to a short introduction to the dynamical calculations. Results are then shown in Section 5, mostly for central $^{197}Au + ^{197}Au$ collisions at $1AGeV$, in terms of pion and kaon yields. The initial presentation of the *absolute* yields is relevant for a detailed discussion as well as for a comparison with theoretical results of other groups and with experimental data of the KaoS and FOPI collaborations. All together this intermediate step is important for testing the reliability of the calculations, since ratios do not do it. Finally we present the pion and strangeness ratios and discuss their dependence on the in-medium modifications of the cross NN cross sections and of the kaon potentials, including the isospin effects. In Section 6 we conclude with a summary and some general comments and perspectives.

2 Theoretical description of the collision dynamics

In this chapter we briefly discuss the transport equation focusing on the treatment of two features important for kaon dynamics: (a) the collision integral by means of the cross sections; (b) the kaon mean field potential and its isospin dependence.

2.1 The RBUU equation

The theoretical description of HICs is based on the semiclassical kinetic theory of statistical mechanics, i.e. the Boltzmann Equation with the Uehling-Uhlenbeck modification of the collision integral [25]. The relativistic analog of this equation is the Relativistic Boltzmann-Uehling-Uhlenbeck (RBUU) equation [26]

$$\left[k^{*\mu}\partial_\mu^x + (k_\nu^* F^{\mu\nu} + M^*\partial_x^\mu M^*)\,\partial_\mu^{k^*}\right] f(x,k^*) = \frac{1}{2(2\pi)^9}$$
$$\times \int \frac{d^3k_2}{E^*_{\mathbf{k}_2}}\frac{d^3k_3}{E^*_{\mathbf{k}_3}}\frac{d^3k_4}{E^*_{\mathbf{k}_4}} W(kk_2|k_3k_4)\left[f_3 f_4 \tilde{f}\tilde{f}_2 - f f_2 \tilde{f}_3\tilde{f}_4\right] \ , \qquad (1)$$

where $f(x,k^*)$ is the single particle distribution function. In the collision term the short-hand notations $f_i \equiv f(x,k_i^*)$ for the particle and $\tilde{f}_i \equiv (1-f(x,k_i^*))$

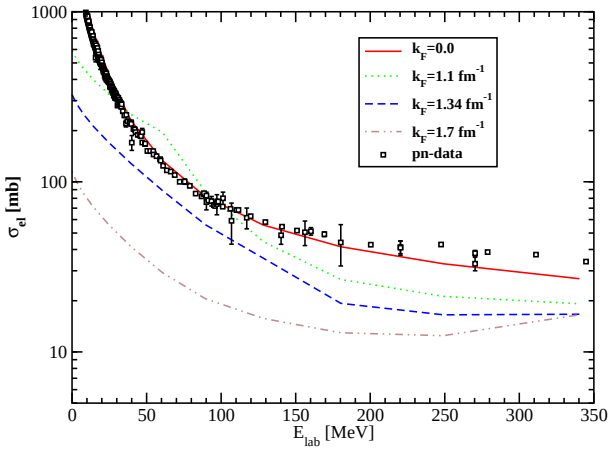

Fig. 1. Elastic in-medium neutron-proton cross section σ_{el} at various Fermi momenta k_F as a function of the laboratory energy E_{lab}. The free cross section ($k_F = 0$) is compared to the experimental total np cross section [17].

for the hole distributions are used, with $E^*_{\mathbf{k}} \equiv \sqrt{M^{*2} + \mathbf{k}^2}$. The collision integral explicitly exhibits the final state Pauli-blocking while the in-medium scattering amplitude includes the Pauli-blocking of intermediate states.

The dynamics of the drift term, i.e. the lhs of eq.(1), is determined by the mean field. Here the attractive scalar field Σ_s enters via the effective mass $M^* = M - \Sigma_s$ and the repulsive vector field Σ_μ via the kinetic momenta $k^*_\mu = k_\mu - \Sigma_\mu$ and via the field tensor $F^{\mu\nu} = \partial^\mu \Sigma^\nu - \partial^\nu \Sigma^\mu$. The dynamical description according to Eq.(1) involves the strangeness propagation in the nuclear medium. This topic will be discussed in more detail at the end of this section.

2.2 In-medium effects on NN cross sections

The in-medium cross sections for 2-body processes (see below) enter in the collision integral via the transition amplitude

$$W = (2\pi)^4 \delta^4 \left(k + k_2 - k_3 - k_4\right) \left(M^*\right)^4 |T|^2 \tag{2}$$

with T the in-medium scattering matrix element.

In the kinetic equation (1) both physical input quantities, the mean field (EoS) and the collision integral (cross sections) should be derived from the same underlying effective two-body interaction in the medium, i.e. the in-medium T-matrix; $\Sigma \sim \Re T \rho_B, \quad \sigma \sim \Im T$, respectively. However, in most practical

applications phenomenological mean fields and cross sections have been used. In such approach the strategy is to adjust to the known bulk properties of nuclear matter around the saturation point, and to try to constrain the models at supra-normal densities with the help of heavy ion reactions [27,28]. Medium modifications of the NN cross sections are usually not taken into account. In spite of that for several observables the comparison to experimental data appears to work astonishingly well [27–30]. However, in particular kinematical regimes a sensitivity to the elastic NN cross sections of dynamical observables, such as collective flows and stopping [19,31] or transverse energy transfer [32], has been observed.

Microscopic Dirac-Brueckner-Hartree-Fock (DBHF) studies for nuclear matter above the Fermi energy regime show a strong density dependence of the elastic [17] and inelastic [18,33] NN cross sections. In such studies one starts from the bare NN-interaction in the spirit of the One-Boson-Exchange (OBE) model by fitting the parameters to empirical nucleon-nucleus scattering and solves then the equations of the nuclear matter many body problem in the T-matrix or ladder approximation. It is not the aim of the present work to go into further details on this topic. An important feature of such microscopic calculations is the inclusion of the Pauli-blocking effect in the *intermediate* scattering states of the T-matrix elements and their in-medium modifications, i.e. the density dependence of the nucleon mass and momenta. Here of particular interest are the in-medium modifications of the inelastic NN cross sections since they directly influence the production mechanism of resonances and thus the creation of pions and kaons according to the channels listed later (see Sect.3). DBHF studies on inelastic NN cross sections are rare and in limited regions of density and momentum [18]. For this reason we will first discuss in the following the in-medium dependence of the elastic NN cross sections, which will be then used as a starting basis for a detailed analysis of the density dependence of the inelastic NN cross sections.

The microscopic in-medium dependence of the elastic cross sections can be seen in Fig. 1, where the energy dependence of the in-medium neutron-proton (np) cross section at Fermi momenta $k_F = 0.0, 1.1, 1.34, 1.7 fm^{-1}$, corresponding to $\rho_B \sim 0, 0.5, 1, 2\rho_0$ ($\rho_0 = 0.16 fm^{-3}$ is the nuclear matter saturation density) is shown. These results are obtained from relativistic Dirac-Brueckner calculations [17]. The presence of the medium leads to a substantial suppression of the cross section which is most pronounced at low laboratory energy $E_{\rm lab}$ and high densities where the Pauli-blocking of intermediate states is most efficient. At larger $E_{\rm lab}$ asymptotic values of 15-20 mb are reached. Also the angular distributions are affected by the presence of the medium. E.g. the initially strongly forward-backward peaked np cross sections become much more isotropic at finite densities, mainly due to the Pauli suppression of intermediate soft modes (π-exchange) [17]. As a consequence a larger transverse energy transfer can be expected.

The case of the inelastic NN cross sections is similar, but more complicated. The presence of the medium influences not only the matrix elements, but also the threshold energy $E_{\rm tr}$, which is an important quantity at beam energies below or near the threshold of particle production. In free space it is calculated from the invariant quantity $s = (p_1^\mu + p_2^\mu)(p_{1\mu} + p_{2\mu})$ with p_i^α, $(i = 1, 2)$ the 4-momenta of the two particles in the ingoing collision channel, e.g. $NN \longrightarrow N\Delta$. This quantity is conserved in binary collisions in free space, from which one determines the modulus of the momenta of the particles in the outgoing channel. The threshold condition reads $E_{\rm tr} \equiv \sqrt{s} \geq M_1 + M_2$. Cross sections in free space are usually parametrized in terms of $\sqrt{s}$ or the corresponding momentum in the laboratory system p_{lab} within the One-Boson-Exchange (OBE) model, see e.g. [34] for details.

At finite density, however, particles carry kinetic momenta and effective masses and obey a dispersion relation $p^*_\mu p^{*\mu} = m^{*2}$ modified with respect to the free case. These in-medium effects shift the threshold energy in the free space according to $s^* = (p_1^{*\mu}+p_2^{*\mu})(p^*_{1\mu}+p^*_{2\mu})$ and the threshold condition for inelastic processes inside the medium reads now $E^*_{\rm tr} \equiv \sqrt{s^*} \geq m_1^*+m_2^*$. The requirement of energy-momentum conservation can be carried out in terms of the quantity s^* *or* s, *only* as long as the in-medium mean fields or the corresponding self energies do not change between ingoing and outgoing channels.

The application of free parametrizations of cross sections for inelastic processes in dynamical situations of HICs at finite density leads thus to an inconsistency, since the threshold condition is performed in terms of effective quantities, but the matrix elements are carried out in free space, e.g. by fitting their parameters to free empirical NN scattering. This effect can be seen in Fig. 2 (left panel) where the free inelastic $NN \longrightarrow N\Delta$ cross section σ_{inel} as a function of the laboratory energy $E_{\rm lab}$ is displayed, at various baryon densities ρ_B. The threshold energy in the free space is $E_{\rm tr} = \sqrt{s} = 2.014$ GeV (for $M = 0.939$ GeV and $M_{min} = 1.076$ for the nucleon and the lower limit mass of the Δ resonance). The corresponding threshold value of the laboratory energy $E_{\rm lab} = (E^2_{\rm tr} - 4M^2)/2M$ is 0.32 GeV. However, at finite density the threshold is shifted towards lower energies, i.e. the free cross section increases, due to the reduction of the free masses of the outgoing particles in the threshold condition $E^*_{\rm tr} \geq m_1^* + m_2^*$. Obviously at higher energies far from threshold the free cross section does not depend on the density.

A more consistent approach is the determination of the inelastic cross section under the consideration of in-medium effects, i.e. the Pauli-blocking of intermediate scattering states and in-medium modified spinors in the determination of the matrix elements within the OBE model. A simultaneous treatment of the transport equation and the structure equations of DBHF for actual anisotropic momentum configurations is not possible, due to its high complexity. For this reason we have applied the same method as for the case

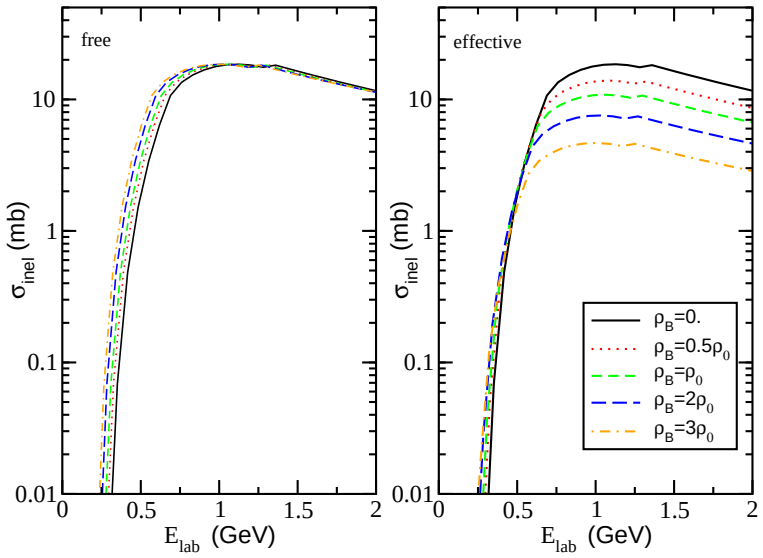

Fig. 2. Inelastic $NN \longrightarrow N\Delta$ cross section σ_{inel} at various baryon densities ρ_B (in units of the saturation density $\rho_0 = 0.16\ fm^{-3}$) as a function of the laboratory energy $E_{\rm lab}$ using the free parametrizations (left) and the in-medium modified ones from DBHF [18] (right).

of elastic binary processes, i.e. in-medium parametrizations of the *inelastic* cross sections of the type $NN \longrightarrow N\Delta$ within the same underlying DBHF approach as already used for the elastic processes. Haar and Malfliet [18] investigated this topic for infinite nuclear matter with the result of a strong in-medium modification of the inelastic cross sections due to the reasons given above. However, these studies were performed at various densities but only in a limited region of momenta. For a practical application in HICs we have thus extended these DBHF calculations using an extrapolation technique. We have imposed an exponential decay law of the form $ae^{-bp_{lab}}$ on the values of the in-medium cross sections of the channel $NN \rightarrow N\Delta$ given in ref. [18]. The parameter a normalizes to the last value of the extrapolated cross section and b is defined by fitting the slope of the free cross section, since it does not change with density. For the density dependence we have enforced a correction of the form $f(\rho_B) = 1 + a_0(\rho_B/\rho_0) + a_1(\rho_B/\rho_0)^2 + a_2(\rho_B/\rho_0)^3$, where $a_0 = -0.601, a_1 = 0223, a_2 = -0.0035$, with ρ_0 saturation density, are extracted from the results of ref.[18]. The same modification is imposed on the cross sections of all the inelastic channels, in a form of the type $\sigma_{eff} = \sigma_{free}(E_{\rm lab})f(\rho_B)$, with σ_{free} taken from the standard free parametrizations of Ref. [34]. Such a procedure is well appropriate at low energies but at higher momenta can be less accurate. This, however, should not be a problem at the reaction energies below the kaon production threshold considered in this work.

Fig. 2 (right panel) shows the energy dependence of the inelastic NN cross section at various densities as obtained from DBHF calculations [17] for sym-

metric nuclear matter. As in the case of elastic processes (see Fig. 1), the inelastic one drops with increasing baryon density ρ_B mainly due to the Pauli blocking of intermediate scattering states and the in-medium modification of the effective Dirac mass [17]. There are also phenomenological studies [16,33] which give similar medium effects on the inelastic cross sections, within the limitation to isospin symmetric nuclear matter. More suitable results would come from a DBHF approach to isospin asymmetric nuclear matter. Only recently such studies have been started [35], however, limiting to low momenta regions, below the threshold energy of inelastic channels.

3 Kaon Potentials

Before starting with the presentation of the results, it is important to analyse the in-medium kaon potential, since it could be relevant when theoretical results will be compared with experiments. In fact it has been widely discussed whether the kaon potential plays a crucial role in describing kaon production and their dynamics [23,7,9]. Kaplan and Nelson [20] found that the explicit chiral symmetry breaking is not so small for K mesons and this leads to significant corrections to the free kaon mass at finite baryon density. There are different models for the description of kaon properties in the nuclear medium. Here we will briefly discuss two main approaches, one based on Chiral Perturbation Theory ($ChPT$) and a second on effective meson couplings (OBE/RMF), more consistent with the general frame of our covariant reaction dynamics. The results are in good agreement and this is not surprising on the basis of a simple physics argument. It is well established [7] that kaons ($K^{0,+}$) feel a weak repulsive potential in nuclear matter, of the order of $20 - 30\ MeV$ at normal density. This can be described as the net result of the cancellation of an attractive scalar and a repulsive vector interaction terms. Such a mechanism can be reproduced in the ChPT approach through the competition between an attractive scalar Kaplan-Nelson term [20] and a repulsive vector Weinberg-Tomozawa [36] term. The same effect can be obtained in an effective meson field scheme just via a coupling to the attractive σ-scalar and to the repulsive ω-vector fields.

In this paper antikaons K^- and their strong attractive potential will be not discussed, since for the higher threshold they have been not considered in the energy range of interest here.

Finally, for studies aimed to the determination of the symmetry energy from strangeness production one has to treat with particular care the isospin dependence of the kaon mean field potential.

3.1 Chiral Perturbative Results

Starting from an effective chiral Lagrangian for the K mesons one obtains a density and isospin dependence for the effective kaon ($K^{0,+}$) masses [7]. In isospin asymmetric matter we finally get

$$m_K^* = \sqrt{m_K^2 - \frac{\Sigma_{KN}}{f_\pi^2}\rho_s \mp \frac{C}{f_\pi^2}\rho_{s3} + V_\mu V^\mu} \qquad (upper\ sign,\ K^+), \qquad (3)$$

where $\rho_s,\ \rho_{s3}$ are total and isospin scalar densities, with $m_K = 494 MeV$ the free kaon mass, $f_\pi = 93 MeV$ the pion decay constant, and Σ_{KN} the kaon-nucleon sigma term (attractive scalar), here chosen as 450 MeV. The vector potential is given by:

$$V_\mu = \frac{3}{8 f_\pi^{*2}} j_\mu \pm \frac{1}{8 f_\pi^{*2}} j_{\mu 3} \qquad (upper\ sign,\ K^+), \qquad (4)$$

with $j_\mu,\ j_{\mu 3}$ baryon and isospin currents. The f_π^* is an in-medium reduced pion decay constant. It is expected to scale with density in a way similar to the chiral condensate [37]. This leads to a reduction around normal density $f_\pi^{*2} \simeq 0.6 f_\pi^2$. Such a reduction is compensated in one-loop ChPT by other contributions in the scalar attractive term so we will use f_π^* only for the vector potential, with an enhanced repulsive effect [7]. The constant C has been fixed from the Gell-Mann-Okubo mass formula (i.e. in free space) to a value of $33.5\, MeV$ [22]. In Eqs. (3-4) upper signs hold for K^+ and lower signs for K^0. As can be seen, the vector term, which dominates over the scalar one at high density, is more repulsive for K^0 than for K^+. This leads to a higher (lower) K^0 (K^+) kaon in-medium energy given by the dispersion relation

$$E_K(\mathbf{k}) = k_0 = \sqrt{\mathbf{k}^2 + m_K^{*2}} + V_0 \qquad (5)$$

The density dependence, evaluated in the chiral approach, of the quantity $E_K(\mathbf{k})_{\mathbf{k}=0} = m_K^* + V_0$ for $K^{0,+}$, that directly influences the in-medium production thresholds is shown by the upper curves in Fig. 3 (left panel). In particular, it can be noted that that K^0 and K^+ in medium-energy differs by $\approx 5\%$ at $\rho_B = 2\rho_0$ (with $E_{K^0} > E_{K^+}$), at a fixed isospin asymmetry around 0.2. Therefore, the inclusion of isovector terms favors K^+ over K^0 production, with a consequent reduction of the K^0/K^+ strangeness ratio.

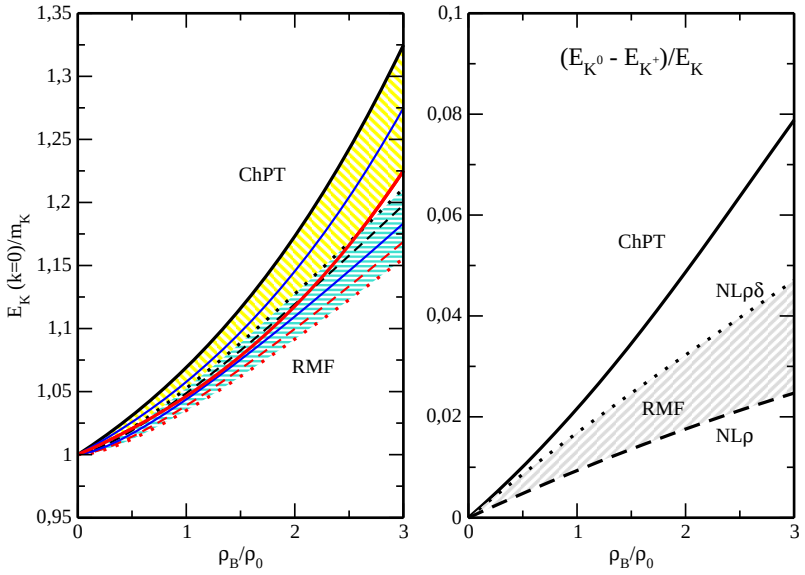

Fig. 3. Density dependence (ρ_0 is the saturation density) of in medium kaon energy (left panel) in unit of the free kaon mass ($m_K = 0.494\,GeV$). Upper curves refer to $ChPT$ model calculations: the central line corresponds to symmetric matter, the other two give the isospin effect (up K^0, down K^+). Bottom curves are obtained in the OBE/RMF approach, the solid one is for symmetric matter. The isospin splitting is given by the dashed ($NL\rho$) and dotted ($NL\rho\delta$) lines, again up K^0, down K^+. Right panel: relative weight of the isospin splitting, see text. All the curves are obtained considering an asymmetry parameter $\alpha = 0.2$.

3.2 Relativistic Mean Field Results

Kaon potentials can be also derived within an effective meson field OBE approach, fully consistent with the RMF transport scheme used to simulate the reaction dynamics, see Eq.(1). We will use a simple constituent quark-counting prescription to relate the kaon-meson couplings to the nucleon-meson couplings, i.e. just a factor 3 reduction. Following the chiral argument discussed before, only for the scalar vector case we have further increased the kaon coupling to $g_{\omega K} \simeq 1.4/3 g_{\omega N}$. This will ensure the required repulsion around normal densities for K^+s. Consistently the isospin dependence will be directly derived from the coupling between the kaon fields and the ρ and δ isovector mesons [22].

The in-medium energy carried by kaons will have the same form as in Eq.(5) but with effective masses and vector potentials given by

$$m_K^* = \sqrt{m_K^2 - m_K(g_{\sigma K}\sigma \pm \frac{g_{\delta K} g_{\delta N}}{m_\delta^2}\rho_{s3})}$$
$$= \sqrt{m_K^2 - m_K(g_{\sigma K}\sigma \pm \frac{1}{3} f_\delta \rho_{s3})} \qquad (6)$$

$$V_0 = \frac{g_{\omega K} g_{\omega N}}{m_\omega^2}\rho_B \pm \frac{g_{\rho K} g_{\rho N}}{m_\rho^2}\rho_{B3}$$
$$= \frac{1}{3}({f_\omega}^*\rho_B \pm f_\rho \rho_{B3}) \quad (7)$$

where upper signs are for K^+s. The $f_i \equiv g_{iN}^2/m_i^2,\ i = \sigma, \omega, \rho, \delta$ are the nucleon-meson coupling constants used in our RMF Lagrangians and $f_\omega^* = 1.4 f_\omega$ due to the enhanced kaon-scalar/vector coupling. σ represents the solution of the non linear equation for the scalar/isoscalar field which gives the reduction of the nucleon mass in symmetric matter, therefore we can directly evaluate the kaon-σ coupling using

$$g_{\sigma K}\sigma = \frac{1}{3}(M - M^*)$$

where M^* is the nucleon effective mass at the fixed baryon density.

In this RMF approach we can derive an almost analytical expression for the isospin effects on the kaon in-medium energy Eq.(5) at $\mathbf{k} = 0$. Using the approximate form $\rho_s \simeq M^*/E_F^*\rho_B$ for the scalar density, we get a relative weight of the isospin splitting of the kaon potentials $\Delta E_K(\mathbf{k})_{\mathbf{k}=0} \equiv E_{K^0}(\mathbf{k})_{\mathbf{k}=0} - E_{K^+}(\mathbf{k})_{\mathbf{k}=0}$ given by

$$\frac{\Delta E_K}{E_K} = \frac{2\alpha(f_\rho - \frac{M^*}{2E_F^*}f_\delta)}{f_\omega^* + \frac{3}{\rho_B}(m_K - \frac{1}{6}(M - M^*))} \quad (8)$$

with $\alpha \equiv \rho_{B3}/\rho_B$ the asymmetry parameter.

We can now easily estimate the isospin splitting of K^0 vs. K^+ for the two isovector mean field Lagrangians used here, $NL\rho$ and $NL\rho\delta$. The effect will be clearly larger when the δ coupling is included since we have to increase the ρ-coupling f_ρ, see [14,15], but still the expected weight is relatively small, going from about 1.5% ($NL\rho$) to about 3.0% ($NL\rho\delta$) at $\rho_B = 2\rho_0$, for a fixed isospin asymmetry around 0.2. The complete results are also shown in Fig. 3 (right panel). The agreement with the ChPT estimations is rather good, but in the RMF scheme we see an overall reduced repulsion and a smaller isospin splitting. Both effects are of interest for our discussion, the first affecting the $K^{0,+}$ absolute yields, the second important for the K^0/K^+ yield ratios.

4 Numerical realization and notations

The Vlasov term of the RBUU equation (1) is treated within the Relativistic Landau-Vlasov method, in which the phase space distribution function $f(x, p^*)$ is represented by covariant Gaussians in coordinate and momentum space [38]. For the nuclear mean field or the corresponding EoS in symmetric matter the

	$f_\sigma\ (fm^2)$	$f_\omega\ (fm^2)$	$f_\rho\ (fm^2)$	$f_\delta\ (fm^2)$	A (fm^{-1})	B	
$NL\rho$	9.3	3.6	1.22	0.0	0.015	-0.004	
$NL\rho\delta$	9.3	3.6	3.4	2.4	0.015	-0.004	

Table 1
Coupling parameters in terms of $f_i \equiv (\frac{g_i}{m_i})^2$ for $i = \sigma,\ \omega,\ \rho,\ \delta$, $A \equiv \frac{a}{g_\sigma^3}$ and $B \equiv \frac{b}{g_\sigma^4}$ for the non-linear NL models [14] using the ρ ($NL\rho$) and both, the ρ and δ mesons ($NL\rho\delta$) for the description of the isovector mean field.

$NL2$ parametrization [26] of the non-linear Walecka model [39] is adopted with a compression modulus of 200 MeV and a Dirac effective mass of $m^* = 0.82\ M$ (M is the bare nucleon mass) at saturation. The momentum dependence enters via the relativistic treatment in terms of the vector component of the baryon self energy. The isovector components in the mean fields are introduced in the $NL\rho, NL\rho\delta$ Lagrangians as in the recent Refs. [14,15]. In Table 1 we report all the coupling constants and the coefficients of the non-linear σ-terms.

The collision integral is treated within the standard parallel ensemble algorithm imposing energy-momentum conservation. For the elastic NN cross sections the DBHF calculations of Ref. [17] have been used throughout this work. At intermediate relativistic energies up to the threshold of kaon ($K^{0,+}$) production, i.e. $E_{lab} = 1.56$ GeV, the major inelastic channels are (B, Y, K stand for a baryon (nucleons N or a Δ-resonance), hyperon and kaon, respectively)

– $NN \longleftrightarrow N\Delta$ (Δ-production and absorption)
– $\Delta \longleftrightarrow \pi N$ (π-production and absorption)
– $BB \longrightarrow BYK$, $B\pi \longrightarrow YK$ (K-production from BB and $B\pi$-channels)

The produced resonances propagate in the same mean field as the nucleons, and their decay is characterized by the energy dependent lifetime Γ which is taken from Ref. [34]. The produced pions propagate under the influence of the Coulomb interaction with the charged hadrons. Kaon production is treated hereby perturbatively due to the low cross sections, taken from Refs. [40]. Kaons undergo elastic scattering and their phase space trajectories are determined by relativistic equations of motion, if the kaon potential is accounted for.

In the next section the results of transport calculations in terms of pion and kaon yields and their rapidity distributions will be presented. The following cases for the inelastic NN cross sections σ_{inel} and the kaon potential Σ_K (scalar and vector) will be particularly discussed:

– free σ_{inel}, without Σ_K (w/o K-pot σ_{free})

– free σ_{inel}, with Σ_K (w K-pot σ_{free})
– free σ_{inel}, with isospin dependent Σ_K (w ID K-pot σ_{free})
– effective σ_{inel}, without Σ_K (w/o K-pot σ_{eff})
– effective σ_{inel}, with Σ_K (w K-pot σ_{eff})
– effective σ_{inel}, with isospin dependent Σ_K (w ID K-pot σ_{eff})

For pions only the different cases of σ_{inel} will be labelled, since they do not experience any potential, apart coulomb. One should note that in all calculations only inelastic processes including the lowest mass resonance $\Delta(1232MeV)$ have been considered, without accounting for the $N^*(1440)$ resonance. This will have not appreciable consequences for pions yields, but it slightly reduces the kaon multiplicities.

5 Results

As mentioned in the introduction, the main topic of the present work is to study the sensitivity of particle ratios to physical parameters such as in-medium effects of cross sections and the isospin dependence of the kaon potential. This is an important issue to clarify since there is some evidence suggesting the yield ratios as good observables in determining the high density behavior of the symmetry energy. In a near future these data will be experimentally accessible with the help of reactions with radioactive ion beams. However, a comparison of absolute values with experimental data, although it is not the aim of this work, is essential and it has to be included in order to show the consistency of our approach. Thus we will start the presentation of the results first in terms of absolute yields, and comparison with data, before passing to the main section on the particle ratios. Most calculations refer to central $^{197}Au + ^{197}Au$ collisions at 1 $AGeV$.

5.1 Effects of in-medium inelastic NN cross sections on particle yields

5.1.1 Resonance and Pion Production

Here we study the role of the density dependence of the effective inelastic NN cross sections on particle yields (pions and kaons). We start with the temporal evolution of the Δ resonances and the produced pions, as shown in Fig. 4. The maximum of the multiplicity of produced Δ-resonances occurs around 15 fm/c which corresponds to the time of maximum compression. Due to their finite lifetimes these resonances decay into pions (and nucleons) as $\Delta \longrightarrow \pi N$. Some of these pions are re-absorbed in the inverse process, i.e. $\pi N \longrightarrow \Delta$ but *chemical equilibrium* is never reached, as pointed out in [15]. This

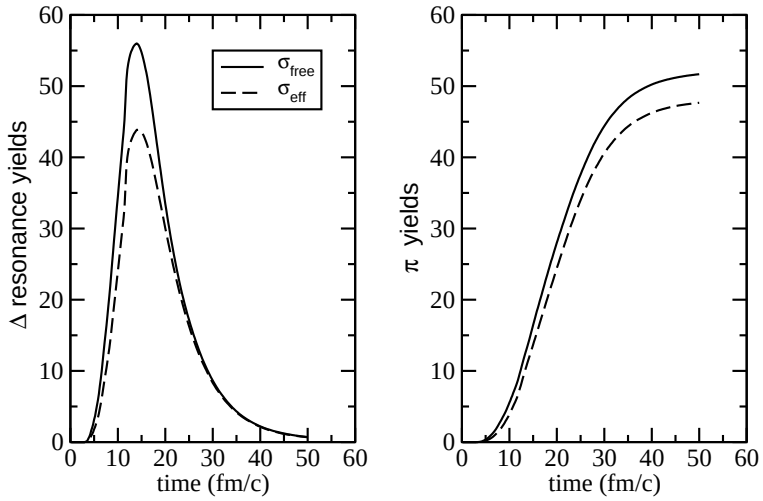

Fig. 4. Time evolution of the Δ-resonances (left panel) and total pion yield (right panel) for a central ($b = 0\ fm$) Au+Au reaction at 1 AGeV incident energy. Calculations with free (solid lines) and effective (DBHF, dashed lines) σ_{inel} are shown.

mechanism continues until all resonances have decayed leading to a saturation of the pion yield for times $t \geq 50$ fm/c (the so-called freeze-out time). The resonance production takes place during the high density phase, where the in-medium effects of the effective cross sections are expected to dominate. In fact, the transport results with the in-medium modified σ_{inel} reduce the multiplicity of inelastic processes, and thus the yields of Δ resonances and pions. However, the in-medium effect is not so pronounced here with respect to similar phenomenological studies of Ref. [16,33], which should come from the moderate density dependence of the effective cross sections, see also again Fig. 2.

Fig. 5 shows the centrality dependence of the charged pion yields for Au+Au collisions at 1.0 AGeV incident energy. The degree of centrality is characterized by the observable A_{part}, which gives the number of participant nucleons and can be calculated within a geometrical picture using smooth density profiles for the nucleus [41]. Obviously A_{part} increases with decreasing impact parameter b and its value approaches the total mass number of the two colliding nuclei in the limiting case of $b = 0$ fm. As can be seen in Fig. 5, the charged pion yields are enhanced with increasing A_{part}, particularly in a non-linear A_{part}-dependence. As pointed out in [41], the charged pion multiplicities show a similar non-linear increase also in the data. However, by directly comparing the theoretical charged pion yields with the experiments [41] we observe that our calculations overpredict the data, even when the in-medium reductions in σ_{inel} are accounted for.

This discrepancy is a general feature of the transport models and may lie on the role of the rescattering processes that take place in the spectator region,

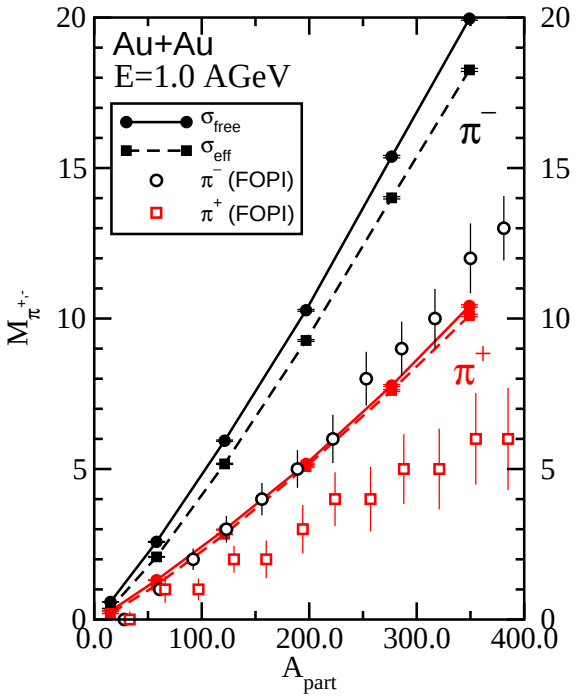

Fig. 5. Centrality dependence (in terms of A_{part}) of the negative (π^-) and positive (π^+) charged pions for Au+Au collisions at 1 AGeV incident energy. Calculations with free (solid lines, filled circles) and effective (dashed lines, filled squares) cross sections are shown as indicated. Experimental data, taken from FOPI collaboration [41], are also displayed for comparison.

where nuclear surface effects can play a crucial role. In order to check this point we have performed a selection on pions produced at central rapidity, where data are also available [41].

In Fig. 6 we present the inclusive (all centralities) pion rapidity distributions vs. the FOPI data for charged pions. We see that the agreement is rather good at mid-rapidity while we see a definite overcounting in the spectator sources.

Such a good evaluation of the pion production ad mid-rapidity is confirmed by the results shown in Fig. 7, where we present the inclusive (all centralities) pion transverse spectrum at midrapidity ($-0.2 < y^0 < 0.2$). We first note that this is also not much affected by the inclusion of the in-medium inelastic cross sections. Moreover we see again that our results are in good agreement with the experimental values from the FOPI collaboration [41], in the same rapidity selection. The overestimation of the pion yields shown in Fig. 5 probably results from other rapidity regions where the role of the spectator sources is more evident. We have also to say that we are not imposing any experimental filter to our results. The point is rather delicate since the main discrepancies appear in high rapidity regions. In any case such a fine agreement at mid-

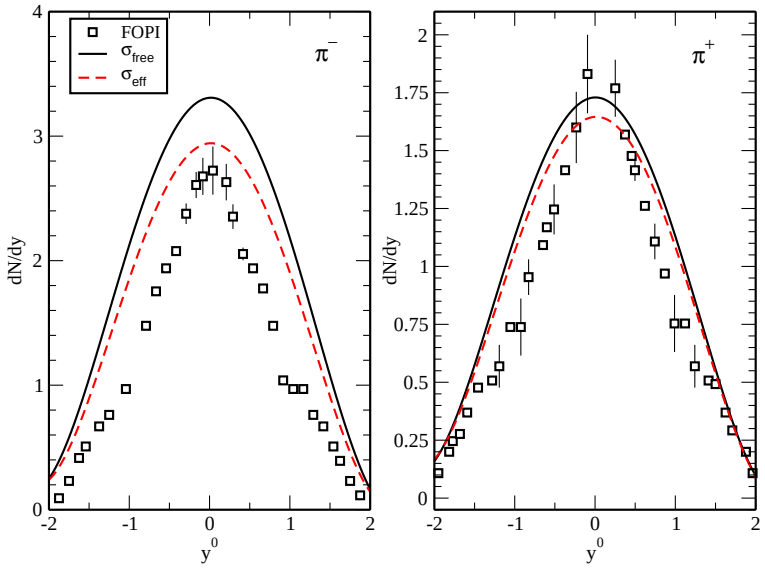

Fig. 6. Inclusive (all centralities) pion rapidity distributions for a Au+Au reaction at $E_{\rm beam} = 1$ AGeV incident energy. Comparison with the experimental values given by FOPI collaboration [41]; as in the data we have used a transverse momentum cut to $p_t > 0.1 GeV/c$.

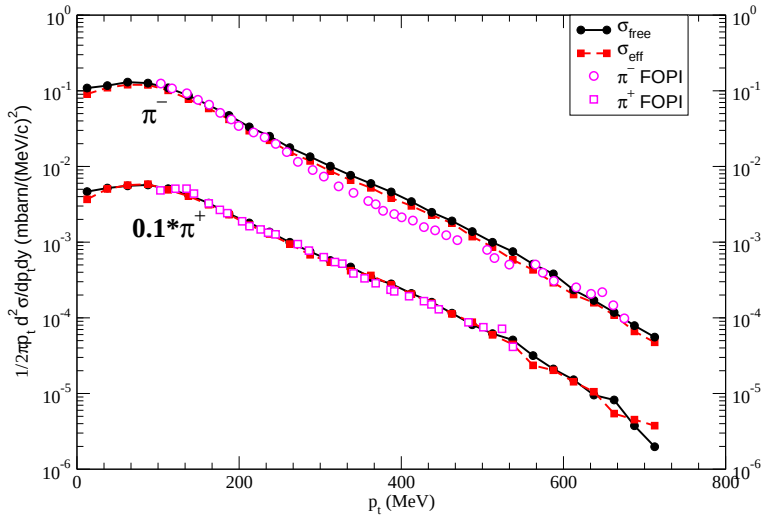

Fig. 7. Inclusive transverse spectrum at midrapidity of π^-, π^+ for a Au+Au reaction at $E_{\rm beam} = 1$ AGeV incident energy. Comparison with the experimental values given by FOPI collaboration [41]. The cross sections are normalized to a rapidity interval $dy = 1$.

rapidity is very important for the reliability of our results on kaon production, mostly produced in that rapidity range via secondary $\pi N, \Delta N$ channels, see [15].

The pion reaction dynamics is furthermore not sensitively affected by the in-medium inelastic cross sections. We restrict here the analysis to *central* Au+Au collisions at 1 AGeV. In Fig. 8 we show cross section effects on the

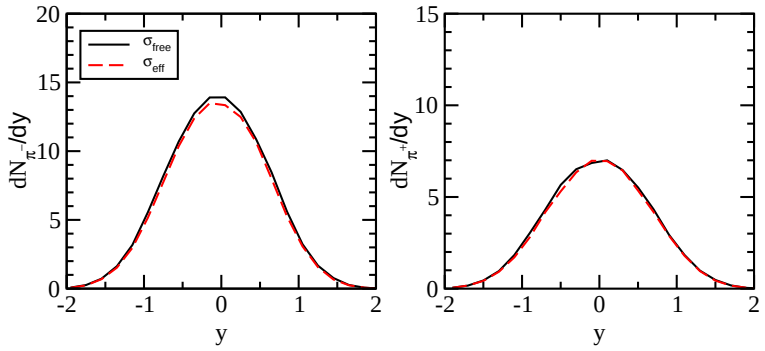

Fig. 8. Rapidity distributions of negative and positive charged pions (left and right panels, respectively) for a central ($b = 0$ fm) Au+Au reaction at $E_{\rm beam} = 1$ AGeV incident energy.

rapidity distributions (normalized to the projectile rapidity in the *cm* system) for $\pi^{\pm}$, an observable which characterizes the degree of stopping or the transparency of the colliding system. This is due to the fact that the global dynamics is mainly governed by the total NN cross sections, in which its elastic contribution is the same for all the cases. In previous studies [19,31] the in-medium effects of the *elastic* NN cross sections gave important contributions to the degree of transparency or stopping. It was found that a reduction of the effective NN cross section particularly at high densities is essential in describing the experimental data [19], as confirmed by various other analyses [31]. The density effects on the inelastic NN cross section influence only those nucleons associated with resonance production, and therefore they do not affect the global baryon dynamics significantly.

5.1.2 Kaon Production

The situation is different for kaon production, see Fig. 9. The influence of the in-medium dependence of σ_{inel} is important, and reduces the kaon abundancies by a factor of $\approx 30\%$. This is due to the fact that the leading channels for kaon production are $N\Delta \longrightarrow BYK$ and $N\pi \longrightarrow \Lambda K$. Thus kaon production is essentially a twostep process and the medium-modified inelastic cross sections enter twice, leading to an increased sensitivity.

Fig. 10 shows the rapidity distributions of kaons, where the in-medium effect is more visible with respect to the corresponding pion rapidity distributions (see Fig. 8). These results seem to show that kaon production could be used to determine the in-medium dependence of the NN cross section for inelas-

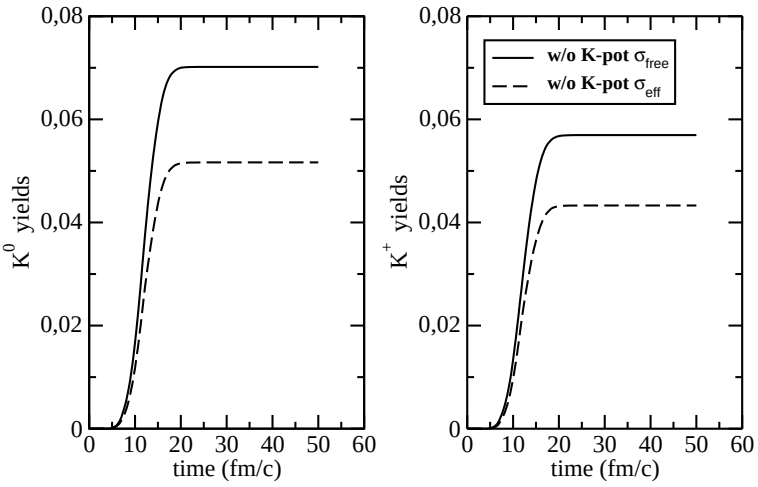

Fig. 9. Time evolution of the K^0 (left panel) and K^+ (right panel) multiplicities, for the same reaction and models as in Fig. 4, with free and in-medium inelastic cross sections, without the inclusion of the kaon potentials.

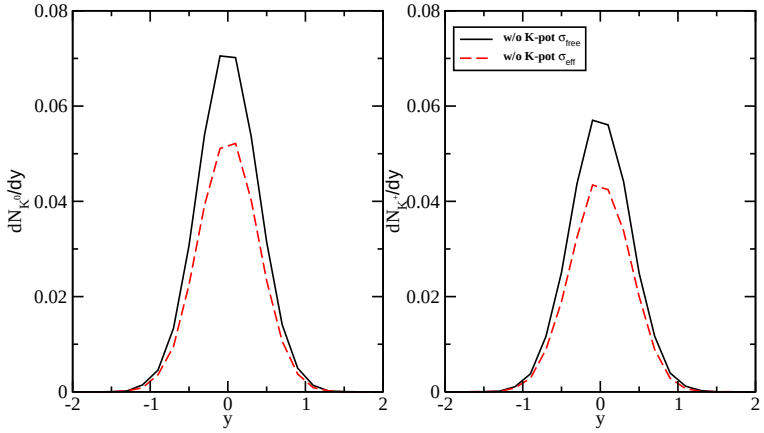

Fig. 10. Same as in Fig. 9, but for the normalized rapidity distributions.

tic processes. Similar phenomenological studies based on the BUU approach [16,33] strongly support in-medium modifications of the free cross sections. It is of great interest to perform an extensive comparison with experimental data on kaon production, in order to have a more clear image of the effect of the in-medium cross sections on their production. The point is that kaon absolute yields are also largely affected by the kaon potentials, see the following, as expected from the general discussion of the previous section. However since kaons are mainly produced in more uniform high density regions the effects of the medium on cross sections tend to disappear in the yield ratios. In the next section we will show that the same holds true for the K^0, K^+ potentials. Our conclusion is that the kaon yield ratios might finally be a rather *robust*

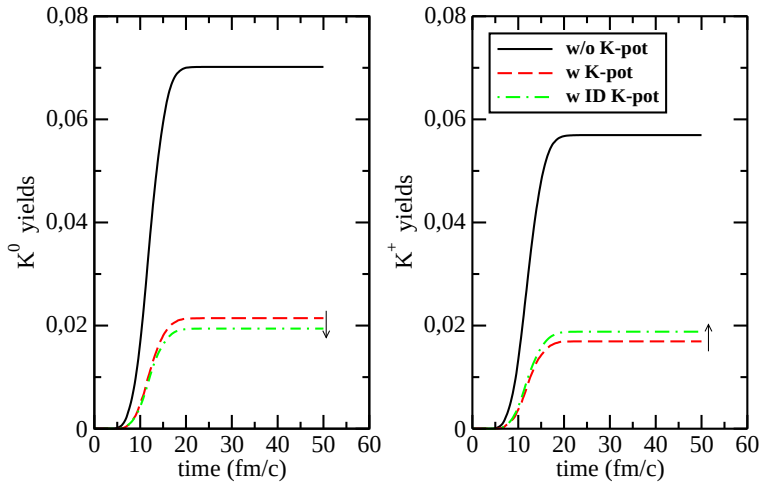

Fig. 11. Time evolution of the K^0 (left panel) and K^+ (right panel) multiplicities for the same reaction as in Fig. 4. Calculations without (w/o K-pot, solid), with (w K-pot, dashed) and with the isospin dependent (w ID K-pot,dotted-dashed) kaon potential are shown. In all the cases the free choice for σ_{inel} is adopted.

observable to probe the nuclear *EoS* at high baryon densities.

5.2 The role of the kaon potential

As discussed in the previous sections, the important quantity which influences the kaon production threshold is the in-medium energy at zero momentum [7]. This quantity rises with increasing baryon density and in the general case of isospin asymmetric matter shows a splitting between K^0 and K^+, see Fig. 3.

We are presenting here several K-production results in *ab initio* collision simulations using the Chiral determination of the K-potentials, *ChPT*. Fig. 11 shows the time dependence of the two isospin states of the kaon with respect to the role of the kaon potential and its isospin dependence. First of all, the repulsive kaon potential considerably reduces the kaon yields, at least in this *ChPT* evaluation.

The inclusion of the isospin dependent part of the kaon potential slightly modifies the kaon yields, towards a larger K^+ production in neutron-excess matter. However by comparing to the corresponding isospin dependence of the in-medium kaon energy, see Fig. 3, the effect is less pronounced in the dynamical situation. This is due to the fact that in heavy ion collisions the local asymmetry in the interacting region varies with time, see [15]. In particular, it decreases with respect to the initial asymmetry because of partial isospin equilibration due to stopping and inelastic processes with associated isospin exchange. This is reflected also in the kaon rapidity distributions, see Fig. 12,

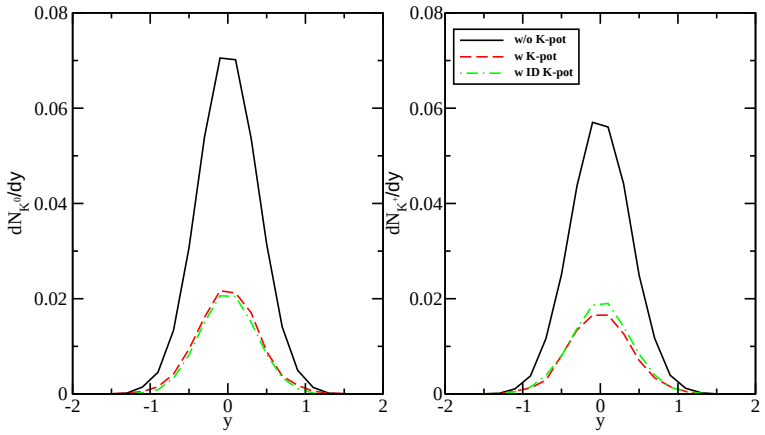

Fig. 12. Same as in Fig. 11, but for the rapidity distributions.

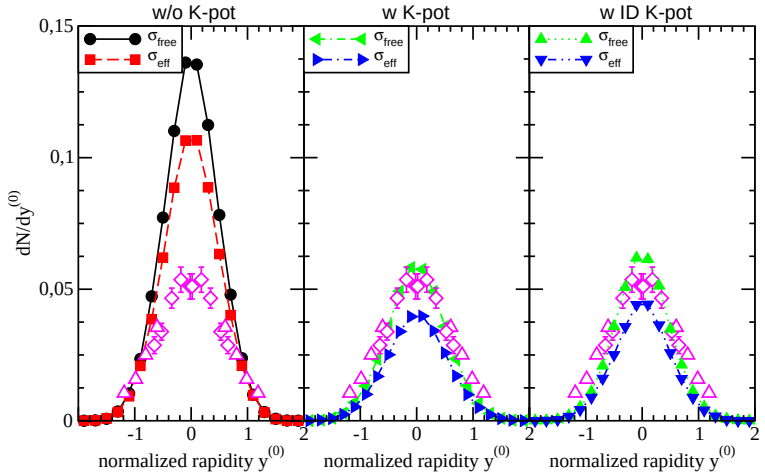

Fig. 13. K^+ rapidity distributions for semi-central($b < 4\ fm$) Ni+Ni reactions at 1.93 AGeV. Theoretical calculations (as indicated) are compared with the experimental data of FOPI (open triangles) and KaoS (open diamonds) collaborations [42,43].

where the role of the kaon potential is crucial, but not its isospin dependence.

As we have already seen even in-medium modifications of inelastic cross sections are affecting the kaon absolute yields, so it appears of interest to look at the combined effects. For that purpose we have performed calculations for a semi-central ($b < 4fm$) Ni+Ni system at $1.93AGeV$, where data are existing from the FOPI [42] and KaoS [43] collaborations. The results for K^+ rapidity distributions, compared to experimental data, are shown in Fig.13.

We observe that although the kaon yields are reduced when using the in-medium inelastic cross section, we are still rather far away from the data, left panel of Fig. 13. We note that the reduction due to the density dependence of the effective inelastic cross sections is rather moderate here with respect to that of the heavier Au-system (see Fig. 10). for kaons). This is due to the less compression achieved for the lighter Ni-systems. The inclusion of the kaon potential, without (central panel) and with (right panel) isospin dependence, is further suppressing the K^+ yield, towards a better agreement with data, as expected for the repulsive behavior at high density.

In fact the results obtained with kaon potentials and effective cross sections seem to underestimate the data. This could be an indication that the $ChPT$ K-potentials are too repulsive at densities around $2\rho_0$ where kaons are produced, see [15]. We like to remind that the parameters of $ChPT$ potentials are essentially derived from free space considerations. When we follow a more consistent RMF approach, directly linked to the effective Lagrangians used to describe bulk properties of the nuclear matter as well as the relativistic transport dynamics, we see less repulsion, bottom curves in Fig. 3 (left panel). This is valid also for the isospin dependent part of the K-potentials, that more directly will affect the K^0/K^+ yield ratio. We see from the same Fig. 3 (right panel) that in the RMF frame this splitting is reduced to a few percent for all the different isovector interactions. The conclusion is that when kaon potentials are evaluated within a consistent effective field approach we have a better agreement with data for absolute yields, with a very similar reduction of the K^0 and K^+ rates. This is important for the yield ratio, that then should be not much sensitive to the in-medium effects on kaon propagation.

A similar conclusion on K-potential effects, obtained within the $ChPT$ approach, can be drawn from the centrality dependence of the K^+ yields shown in Fig. 14 in the case of Au+Au collisions at 1 AGeV beam energy and compared with KaoS data [44]. The trend in centrality can be reproduced by all theoretical calculations (with different cross sections), however, all of them seem to underestimate the experimental yields.

In fact we have to mention that another possible source of the discrepancy with data can be that in all our simulations only the lowest mass resonance $\Delta(1232MeV)$ has been dynamically included. Transport calculations from other groups, that take care also of the $N^*(1440MeV)$ resonance, are getting an enhancement of the K^+ yield for Au+Au collisions at 1 AGeV incident energy [7]. This significant dependence of the kaon yields on the N^* resonance comes from the 2-pionic N^*-decay channel, i.e. $N^* \longrightarrow \pi\pi N$. Therefore, since the most important channels of kaon production are the pionic ones, we can expect some underestimation of the absolute yields in our calculations. Just to confirm this point, in Fig. 14 we report also transport results from the Tübingen group, in which all resonances are accounted for [7]. We finally re-

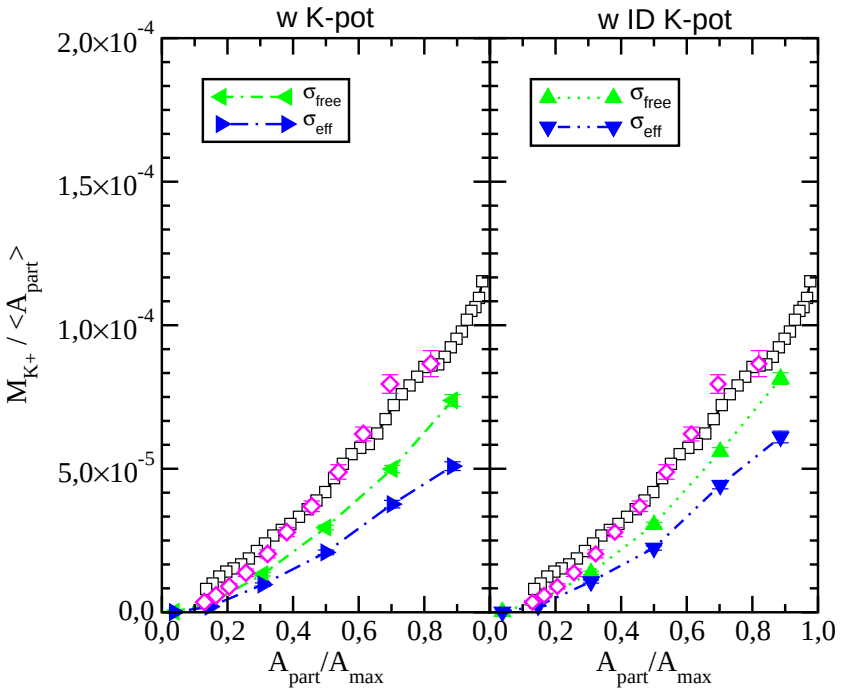

Fig. 14. K^+ centrality dependence in Au+Au reactions at 1 AGeV incident energy. Our theoretical calculations (as indicated) are compared with KaoS data from [44] (open diamonds) and with results of the Tübingen group (open squares).

mark that the inclusion of other nucleon resonances in neutron-rich matter will further contribute to increase the K^0 yield through a larger intermediate $\pi-$ production. This can contribute to compensate the opposite effect of isospin dependent part of the K-potentials on the K^0/K^+ yield ratios.

5.3 Pionic and Strangeness Ratios

A crucial question is whether particle yield *ratios* are influenced by in-medium effects both on inelastic cross section and kaon potentials. This point is of major importance particularly for kaons, since ratios of particles with strangeness have been widely used in determining the nuclear EoS at supra-normal density. Relative ratios of kaons between different colliding systems have been utilized in determining the isoscalar sector of the nuclear EoS [5]. More recently, the (π^-/π^+)- and (K^0/K^+)-ratios have been proposed in order to explore the high density behavior of the symmetry energy, i.e. the isovector part of the nuclear mean field [14,15,13,12].

Fig. 15 shows the incident energy dependence of the pionic (π^-/π^+, left panel) and strangeness (K^0/K^+, right panel) ratios for the different choices of inelastic cross sections and kaon potentials, as widely discussed in the previous sections.

First of all, a rapid decrease of the pionic ratio with increasing beam energy

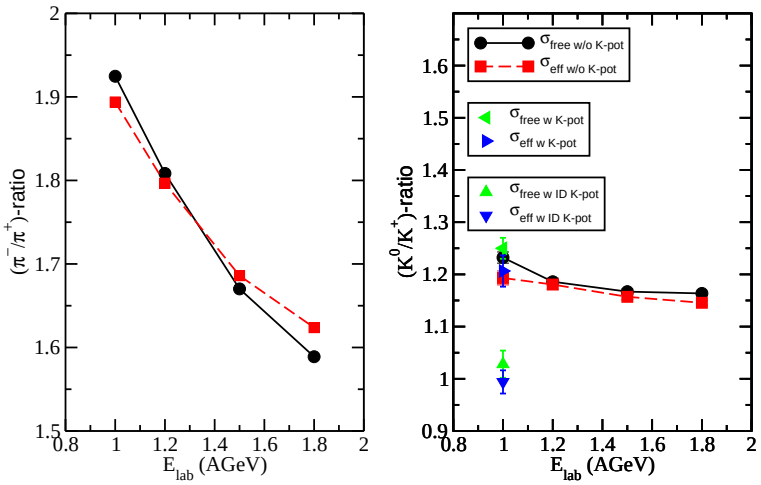

Fig. 15. Energy dependence of the π^-/π^+ (left panel) and K^0/K^+ (right panel) ratios for central ($b = 0$ fm) Au+Au reactions.

is observed, related to the opening of secondary rescattering processes (reabsorption/recreation of pions with associated isospin exchange) channels. The corresponding strangeness ratio depends only moderately on beam energy due to the absence of secondary interactions with the hadronic environment.

The pionic ratio is partially affected by the in-medium effects of σ_{inel}, as it can be seen in the left panel of Fig.15. Its slope is slightly changing with respect to beam energy. The situation is similar for the strangeness ratio, which actually appears even more *robust* vs. in-medium modifications, even with the kaon potentials. This can be seen in the right panel of Fig.15, where for all the considered beam energies the ratio remains almost unchanged. Such a result is consistent with those of the previous sections, where it was found that the absolute kaon yields decrease in the same way when the effective σ_{inel} are applied and when the K-potentials are included.

The different sensitivity to variations in the inelastic cross sections of pionic vs. strangeness ratios can be easily understood. For the large rescattering and lower masses pions can be produced at different times during the collision, in different density regions. At variance kaons are mainly produced at early times in a rather well definite compression stage, i.e. in a source with a more uniform high density, and so the density dependence of the inelastic cross sections will affect in the same way neutral and charged kaon yields, leaving the ratio unchanged. At this level of investigation one could argue that the strangeness ratio is a very promising observable in determining the nuclear EoS and particularly its isospin dependent part. This has been also the main conclusion in Ref. [15].

However, a strong isospin dependence of the kaon potentials could directly

	NL	$NL\rho$	$NL\rho\delta$
K^0/K^+ (w/o K-pot)	1.24 ($\pm$ 0.02)	1.35 ($\pm$ 0.01)	1.43 ($\pm$ 0.02)
K^0/K^+ (w ID K-pot)	1.02 ($\pm$ 0.03)	1.22 ($\pm$ 0.04)	1.34 ($\pm$ 0.05)

Table 2
Sensitivity of the strangeness ratio K^0/K^+ to the isospin dependent kaon potential and to the isovector mean field (NL, no isovector fields, $NL\rho$ and $NL\rho\delta$). The considered reaction is a central (b = 0 fm) Au+Au collision at 1 AGeV incident energy.

affect the ratio, since the K^0 and K^+ rates will be modified in opposite ways. This is shown by the two triangle points at 1 AGeV in the right panel of Fig. 15. As already discussed this large isospin dependence of the kaon potential, clearly present in the $ChPT$ evaluation, is greatly reduced in a consistent mean field approach, see Fig. 3 and the arguments presented in Section 3. In any case this point deserves more detailed studies. We plan to perform *ab initio* kaon-production simulations within the OBE/RMF evaluation of kaon potentials, with an isospin part fully consistent with the isovector fields of the Hadronic Lagrangians used for the reaction dynamics.

An interesting final comment is that the sensitivity of the strangeness ratio to the isovector part of the nuclear EoS remains even when strong isospin dependence of the kaon potentials is inserted, as in the $ChPT$ case.

In order to check this, we have repeated for Au+Au at 1 AGeV incident energy the calculations by varying the isovector part of the nuclear mean field. As in Refs. [14,15], three options for the isovector mean field have been applied: the NL (no isovector fields), $NL\rho$ and $NL\rho\delta$ parametrizations, but now including the isospin effect in the kaon potential in the $ChPT$ evaluation. The options of the symmetry energy differ from each other in the high density stiffness. NL gives a relatively soft E_{sym}, $NL\rho\delta$ a relatively stiff one, and $NL\rho$ lies in the middle between the other limiting cases [14]. Table 2 shows the strangeness ratio as function of these different cases for the isovector mean field, keeping now constant the other parameters (free σ_{inel}, isospin dependent kaon potential). The ratio, indeed, strongly decreases when the isospin part in the kaon potential is accounted for. The more interesting result is, however, that the relative difference between the different choices of the symmetry energy remains stable. This can be understood from the fact that in the kaon self energies the isospin sector contains only the isospin densities and currents without additional parameters such meson-nucleon coupling constants. Since the local asymmetry does not strongly vary from one case to the other (NL, $NL\rho$, $NL\rho\delta$), one would expect a robustness of the EoS dependence. Thus we conclude that the strangeness ratio appears to be well suited in determin-

ing the isovector EoS, however, a fully consistent mean field approach is still missing.

6 Conclusions

We have investigated the role of the in-medium modifications of the inelastic cross section and of the kaon mean field potentials on particle production in intermediate energy heavy ion collisions within a covariant transport equation of a Boltzmann type. We have used for both, the elastic and inelastic NN cross sections the same DBHF approach which provide in a parameter free manner the in-medium modifications of the imaginary part of the self energy in nuclear matter. The kaon potential has been evaluated in two ways, following a Chiral Perturbative approach and an Effective Field scheme, considering valence quark-meson couplings. We have applied these modifications of the cross sections and kaon potentials to the collision integral of the transport equation and analyzed Au+Au and Ni+Ni collisions at intermediate relativistic energies around the kaon threshold energy.

Our studies have shown a good sensitivity of the particle multiplicities and rapidity distributions of pions and kaons. In particular, a moderate reduction for pions has been seen when the in-medium effects in the inelastic cross section are accounted for. The pion yields are still overestimating the inclusive data while we have a very nice agreement with the pion spectra and multiplicities at mid-rapidity. The latter point is important for trusting the kaon production, mainly due to secondary pion collisions at mid-rapidity.

At variance the kaon ($K^{0,+}$) yields show a larger sensitivity to the reduction of the inelastic cross sections, with a decrease of about 30 %. However we see that the introduction of a repulsive kaon potential is essential in order to reproduce even inclusive data.

We have then focused our attention on π^-/π^+ and K^0/K^+ yield ratios, recently suggested as good probes of the isovector part of the EoS at high densities. The pionic ratios, due to their strong secondary interaction processes with the hadronic environment, show a dependence on the density behavior of the inelastic cross sections. A further selection of the production source, i.e. a transverse momentum discrimination, could be required in order to have a more reliable probe of the nuclear EoS.

The situation appears more favorable for the kaon ratios. In fact we find that the multiplicities of K^0 and K^+ are influenced in such a way that their ratio is not affected by the density dependence of the inelastic cross sections. This is due to the long mean free path of the $K^{0,+}$ that are produced only in the

compression stage of the collision [15]. The effects of the in medium kaon potentials are also largely compensating in the K^0/K^+ yield ratio, due to the similar repulsive field seen by K^0 and K^+ mesons. Such a result can be modified by the isospin dependence of the kaon potentials which is expected to act in opposite directions for neutral and charged kaons rates. Actually this is a rather stimulating open problem. In our analysis with two completely different approaches, $ChPT$ vs. RMF, we get a good agreement for the isoscalar kaon potential but a rather different prediction for the isovector part.

However, a study in terms of the different choices of the isovector kaon field has shown that the relative dependence of the strangeness ratios on the stiffness of the isovector nuclear EoS remains a well robust observable. This is an important issue in determining the high density behavior of the symmetry energy in more systematic analyses in the future, when more experimental data will be available.

Acknowledgments. This work is supported by BMBF, grant 06LM189 and the State Scholarships Foundation (I.K.Y.). It is also co-funded by European Union Social Fund and National funded Pythagoras II - EPEAEK II, under project 80861. One of the authors (V.P.) would like to thank H.H. Wolter and M. Di Toro for the warm hospitality during her short stays at their institutes.

References

[1] J. M. Lattimer, M.Prakash, Nucl. Phys **A777**, (2006) 479 and refs. therein; B. Liu, H. Guo, V. Greco, U. Lombardo, M. Di Toro and Cai-Dian Lue, Eur. Phys. J. **A22**, (2004) 337.

[2] T.Klähn et al., Phys. Rev. **C74**, (2006) 035802.

[3] P. Danielewicz, R. Lacey, W.G. Lynch, Science **298**, (2002) 1592

[4] N. Hermann, J.P. Wessels, T. Wienold, Annu. Rev. Nucl. Part. Sci. **49**, (1999) 581.

[5] C. Fuchs et al., Phys. Rev. Lett. **86**, (2001) 1974.

[6] A.B. Larionov, U. Mosel, Phys. Rev. **C72**, (2005) 014901.

[7] C. Fuchs, Prog. Part. Nucl. Phys. **56**, (2006) 1.

[8] J. Aichelin, C.M. Ko, Phys. Rev. Lett. **55**, (1985) 2661.

[9] C. Hartnack, H. Oeschler, J. Aichelin, Phys. Rev. Lett. **90**, (2003) 102302.

[10] C. Sturm et al. (KaoS Collaboration), Phys. Rev. Lett. **86**, (2001) 39.

[11] A. Andronic et al. (FOPI Collaboration), Phys. Lett. **B612**, (2005) 173.

[12] Bao-An Li, Phys.Rev.**C71**, (2005) 014608.

[13] Qing-feng Li, Zhu-xia Li, En-guang Zhao, Raj K. Gupta, Phys. Rev. **C71**, (2005) 054907.

[14] G. Ferini, M. Colonna, T. Gaitanos, M. Di Toro, Nucl. Phys. **A762**, (2005) 147-166.

[15] G. Ferini, T. Gaitanos, M. Colonna, M. Di Toro, H.H. Wolter, Phys. Rev. Lett. **97**, (2006) 202301..

[16] A.B. Larionov, W. Cassing, S. Leupold, U. Mosel, Nucl.Phys. **A696**, (2001) 747.

[17] C. Fuchs et al., Phys. Rev. **C 64**, (2001) 024003.

[18] B. Ter Haar, R. Malfliet, Phys. Rev. **C36**, (1987) 1611.

[19] T. Gaitanos, C. Fuchs, H.H. Wolter, Phys. Lett. **B609**, (2005) 241;
E. Santini, T. Gaitanos, M. Colonna, M. Di Toro, Nucl. Phys. **A756**, (2005) 468;
T. Gaitanos, C. Fuchs, H.H. Wolter, Prog. Part. Nucl. Phys. **53**, (2004) 45.

[20] D.B. Kaplan, A.E. Nelson, Phys. Lett. **B175**, (1986) 57;
A.E. Nelson, D.B. Kaplan, Phys. Lett. **B192**, (1987) 193.

[21] G.Q. Li, C.H. Lee, G.E. Brown, Nucl. Phys. **A625**, (1997) 372.

[22] J. Schaffner-Bielich, I.N. Mishustin, J. Bondorf, Nucl. Phys. **A625**, (1997) 325.

[23] E.L. Bratkovskaya, W. Cassing, U. Mosel, Nucl. Phys. **A622**, (1997) 593.

[24] X. Lopez et al. (FOPI Collaboration), submitted for publication.

[25] L.P. Kadanoff, G. Baym, *Quantum Statistical Mechanics* (Benjamin, New York, 1962).

[26] B. Blättel, V. Koch, U. Mosel, Rep. Prog. Phys. **56**, (1993) 1.

[27] P. Danielewicz, Nucl. Phys. **A 673**, 375 (2000).

[28] A.B. Larionov et al., Phys. Rev. **C62**, 064611 (2000).

[29] T. Gaitanos, C. Fuchs, H.H. Wolter, Amand Faessler, Eur.Phys.J. **A12**, (2001) 421.

[30] T. Gaitanos, C. Fuchs, H.H. Wolter, Nucl.Phys. **A741**, (2004) 287.

[31] D. Persam, C. Gale, Phys. Rev. **C65**, (2002) 064611.

[32] P. Danielewicz, Acta Phys. Polon. **B33**, (2002) 45.

[33] A.B. Larionov, U. Mosel, Nucl.Phys. **A728**, (2003) 135.

[34] H. Huber, J. Aichelin, Nucl. Phys. **A573**, (1994) 587.

[35] E.N.E. van Dalen, C. Fuchs, Amand Faessler, Phys, Rev. **C72**, (2005) 065803.

[36] S. Weinberg, Phys. Rev. **166**, (1968) 1568.

[37] G.E.Brown, M.Rho, Nucl. Phys. **A596**, (1996) 503.

[38] C. Fuchs, H.H. Wolter, Nucl. Phys. **A589**, (1995) 732.

[39] J.D. Walecka, Ann. Phys. (N.Y.) **83**, (1974) 491.

[40] K. Tsushima, A. Sibirtsev, A.W. Thomas, G.Q. Li, Phys. Rev. **C59**, (1999) 369;
K. Tsushima, S.W. Huang, Amand Faessler, Phys. Lett. **B337**, (1994) 245; Austral. J. Phys. **50**, (1997) 35 (nucl-th/9602005).

[41] D. Pelte et al., Z. Phys. **A357**, (1997) 215;
More precise pion data have been recently published in W. Reisdorf et. al., FOPI Collaboration, Nucl. Phys. **A781** (2007) 459.

[42] D. Best et al. (FOPI collaboration), Nucl. Phys. **A625**, (1997) 307

[43] M. Menzel et al. (KaoS collaboration), Phys. Lett. **B495**, (2000) 26.

[44] R. Barth et al. (KaoS collaboration), Phys. Rev. Lett. **78**, (1997) 4007;
P. Senger, H. Ströbele, J. Phys. **G25**, (1999) R59.